

Diffusion-sensitized Ophthalmic MRI Free of Geometric Distortion in Patients with Intraocular Masses

Katharina Paul¹, Andreas Graessl¹, Jan Rieger^{1,2}, Dariusz Lysiak^{1,2}, Till Huelnhagen¹, Lukas Winter¹, Robin Heidemann³, Tobias Lindner⁴, Stefan Hadlich⁵, Annette Zimpfer⁶, Andreas Pohlmann¹, Paul-Christian Krueger³, Soenke Langner³, Oliver Stachs^{4,7}, and Thoralf Niendorf^{1,8}

¹Max-Delbrueck Centre for Molecular Medicine, Berlin Ultrahigh Field Facility (B.U.F.F.), Berlin, Berlin, Germany, ²MRI-TOOLS GmbH, Berlin, Germany, ³Siemens Healthcare Sector, Erlangen, Germany, ⁴University Medicine Rostock, Pre-clinical Imaging Research Group, Rostock, Germany, ⁵University of Greifswald, Institute for Diagnostic Radiology and Neuroradiology, Greifswald, Germany, ⁶University Medicine Rostock, Institute of Pathology, Rostock, Germany, ⁷University Medicine Rostock, Department of Ophthalmology, Rostock, Germany, ⁸Experimental and Clinical Research Center, a joint cooperation between the Charité Medical Faculty and the Max-Delbrueck-Center, Berlin, Germany

Target audience: This work is of interest for basic MR researchers, imaging scientists and clinical scientists.

Purpose: Magnetic resonance imaging (MRI) of the spatial arrangements of the eye segments and their masses is an emerging application which is increasingly used in basic research, (pre)-clinical imaging and diagnostic radiology¹⁻⁵. Diffusion-weighted MRI (DWI) probes self-diffusion of water in tissue on a microscopic level and holds the promise of enhanced diagnostic accuracy over morphological MRI⁶. In today's clinical practice single-shot echo planar imaging (ss-EPI) is most widely employed for neurovascular DWI. However, ss-EPI is prone to magnetic susceptibility artifacts that manifest themselves as signal loss and image distortion. These detrimental effects are more severe at high field strengths, and particularly pronounced in regions with poor main magnetic field (B_0) homogeneity. This constraint constitutes a severe challenge for diffusion-sensitized EPI of the eye and orbit⁷. It has been shown that diffusion-sensitized multi-shot split-echo RARE⁸ (ms-RARE) provides distortion free diffusion weighted images of the eye and orbit at 3.0 T and at 7.0 T⁹. Recognizing the capabilities of ms-RARE, this work examines the applicability of ms-RARE in a small patient cohort including patients with uveal melanoma and/or retinal detachment.

Methods: In vivo studies were performed on a 3.0 T and on a 7.0 T whole body MR system (Siemens Healthcare, Erlangen, Germany). At 3.0 T a body volume RF coil was used for signal transmission and a 32-element head coil (Siemens Healthcare, Erlangen, Germany) was applied for signal reception. A dedicated six-element transceiver coil array consisting of loop elements was employed for in vivo ophthalmic measurements at 7.0 T¹⁰. Informed written consent was obtained from each patient prior to the study in compliance with the local institutional review board guidelines. Patients with uveal melanoma and/or retinal detachment were examined ($n = 6$, mean age: (55 ± 12) years, 4 males, 2 females, mean BMI: (27.5 ± 4.7) kg/m²). T_1 -weighted 3D FLASH imaging was conducted at 3.0 T: TR = 7.6 ms, TE = 2.1 ms, receiver bandwidth = 164 kHz, spatial resolution = $(0.6 \times 0.6 \times 0.6)$ mm³. At 3.0 T diffusion-sensitized ms-RARE was performed using: TR = 4000 ms, TE = 96 ms, receiver bandwidth = 250 kHz, ESP = 4.84 ms, spatial resolution = $(0.5 \times 0.5 \times 5)$ mm³. High-resolution anatomical RARE imaging was conducted at 7.0 T (TR = 2940 ms, TE = 54 ms, receiver bandwidth = 452 kHz, ESP = 17.8 ms, 4 averages) to obtain an anatomical reference with a $(0.1 \times 0.1 \times 1.2)$ mm³ spatial resolution. In one case the diseased eye was enucleated as part of the therapy and afterwards imaged at 9.4 T. For this purpose, ex vivo measurements were conducted on a 9.4 T small bore MR system (Biospec 94/20, Bruker Biospin, Ettlingen, Germany) equipped with a birdcage resonator. Ex vivo anatomical FLASH imaging was performed at 9.4 T: TR = 120 ms, TE = 12.3 ms, receiver bandwidth = 30 kHz, spatial resolution = $(0.05 \times 0.05 \times 0.25)$ mm³, 280 averages. Diffusion-weighted data using spin echo imaging were acquired: TR = 2300 ms, TE = 27.5 ms, receiver bandwidth = 50 kHz, spatial resolution = $(0.1 \times 0.1 \times 0.3)$ mm³, 12 averages. After ex vivo MRI the enucleated globe was fixed in 4% formalin solution for at least 24 hrs and sliced in anterior-posterior direction. A macrophotography of the enucleated and bisected eye was produced. Optical microscopy of H&E stainings was conducted.

Results: Figure 1 summarizes the results for an exemplary patient. A reconstructed slice of the 3D T_1 -weighted anatomical scan (Fig. 1a) and the T_2 -weighted RARE image acquired at 7.0 T (Fig. 1b) of the pathological eye clearly show the loss in integrity of the vitreous compartment as a result of retinal detachment. The in vivo ADC map (Fig. 1c) clearly delineates the hypointense tumor from the surrounding modest hypointense hemorrhage and the hyperintense vitreous body. Mean ADC of the tumor was $(0.97 \pm 0.15) \cdot 10^{-3}$ mm²/s. The subretinal hemorrhage showed an ADC of $(1.67 \pm 0.10) \cdot 10^{-3}$ mm²/s. The vitreous body yielded an ADC of $(2.91 \pm 0.10) \cdot 10^{-3}$ mm²/s. These ADC differences induced an ample contrast between the subretinal hemorrhage and the tumor. Unlike diffusion-weighted ms-RARE and the ADC maps derived from diffusion-weighted ms-RARE the tumor remained undetectable in the high spatial resolution T_1 -weighted anatomical data as well as in the T_2 -weighted RARE image. Ex vivo imaging using FLASH at 9.4 T (Fig. 1d) increases spatial resolution by a factor of 19 compared to in vivo T_2 -weighted imaging at 7.0 T (Fig. 1b). Ex vivo, retinal detachment as well as the tumor itself can be clearly depicted. The fine structure of the tumor is even more pronounced when using high spatial resolution diffusion-weighted MR microscopy at 9.4 T (Fig. 1e). Although the voxel size of the in vivo ADC map acquired at 3.0 T (Fig. 1c) was 2000 times larger compared to that of the ex vivo MR microscopy (Fig. 1f), the ocular mass was still clearly identifiable in the in vivo ADC map (Fig. 1c). Macrophotography of the enucleated eye confirmed the retinal detachment and the extent of the tumor. Histology confirmed the malignancy of the melanoma and its diverse tissue composition including the presence of intratumoral hemorrhage, lymphoid vessels and interlaced fiber bundles as demonstrated by ADC mapping in and ex vivo.

Discussion: RARE-based techniques offer immunity to B_0 inhomogeneities and hence are particularly suited for ophthalmic DWI. This is of clinical relevance since single-shot echo planar imaging – which is commonly used for DWI in today's clinical practice – is prone to magnetic susceptibility artifacts induced by the air filled nasal cavities and frontal sinuses surrounding the eye. Multi-shot RAREs quality and geometric fidelity underscores its value for advancing the capabilities of DWI of the eye and orbit. MRI of subtle ocular structures requires a millimeter to sub-millimeter in-plane spatial resolution over a small field of view (FOV). It has been shown in this study that diffusion-sensitized ms-RARE provides means to distinguish between retinal detachment and ocular mass; a fact that has not been seen in T_1 - and T_2 -weighted anatomical images. This finding underlines the value of distortion-free diffusion-weighted ocular imaging which adds profound clinically relevant information versus conventional anatomic imaging.

Conclusion: This study showed that diffusion-sensitized ms-RARE has the capability to provide distortion-free images of the eye and orbit in patients with uveal melanoma and/or retinal detachment. The obtained in vivo results are confirmed by high-resolution ex vivo MR microscopy and by histology. Notwithstanding the significantly increased voxel size used in our in vivo versus the ex vivo imaging sessions, the in vivo data accord very well with the ex vivo findings and demonstrate the high geometric fidelity and value of in vivo ophthalmic DWI using ms-RARE.

References: [1] Mafee et al, *Neuroimag Clin N Am* 2005, 15:23; [2] Apushkin et al, *Neuroimag Clin N Am* 2005, 15:49; [3] Sepahdari et al, *AJNR* 2012, 33:314; [4] Beenakker et al, *NMR Biomed* 2013, 26:1864; [5] Graessl et al, *Invest Radiol* 2014, 49:260; [6] Norris et al, *NMR Biomed* 1994, 7:304; [7] Erb-Eigner et al, *Invest Radiol* 2013, 48:10; [8] Williams et al, *Magn Reson Med* 1999, 41:734; [9] Fuchs et al, *Proc. Intl. Soc. Mag. Reson. Med.* (22) 2014, 994; [10] Graessl et al, *Invest Radiol* 2014, 49:260.

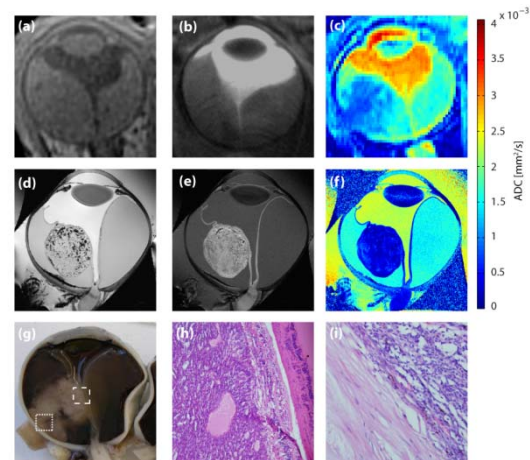


Figure 1: Comparison of in vivo MR imaging at 3.0 T and 7.0 T (a-c), ex vivo MR microscopy at 9.4 T (d-f), macroscopy (g) and histology (h-i). (a): In vivo T_1 -weighted FLASH image acquired in vivo at 3.0 T exhibiting a spatial resolution of $(0.6 \times 0.6 \times 0.6)$ mm³. (b): In vivo T_2 -weighted ms-RARE image obtained at 7.0 T with a spatial resolution of $(0.1 \times 0.1 \times 1.2)$ mm³. (c): In vivo ADC map acquired in vivo at 3.0 T with a spatial resolution of $(0.5 \times 0.5 \times 5)$ mm³. (d): Ex vivo T_2 -weighted FLASH image acquired at 9.4 T exhibiting a spatial resolution of $(0.05 \times 0.05 \times 0.25)$ mm³. (e): Ex vivo diffusion-sensitized ($b = 500$ s/mm²) spin echo image acquired at 9.4 T with a spatial resolution of $(0.1 \times 0.1 \times 0.3)$ mm³. (f): Corresponding ex vivo ADC map exhibiting the same scaling as the in vivo map. (g): Macrophotography of the enucleated eye. (h): H&E staining with 10-fold magnification showing the transition from the ocular mass to the detached retina (dashed box in (g)). (i): H&E staining with 20-fold magnification showing the transition from the sclera to the tumor (dotted box in (g)).